AD-A039 860 FLORIDA UNIV GAINESVILLE DEPT OF PHYSICS F/G 20/8
A SPHERICAL PLATE ELECTROSTATIC ENERGY ANALYZER.(U)
FEB 77 J M PEREZ, T L BAILEY N00014-76-C-0127
UNCLASSIFIED TR-13 NL

| OF |
AD
A039860

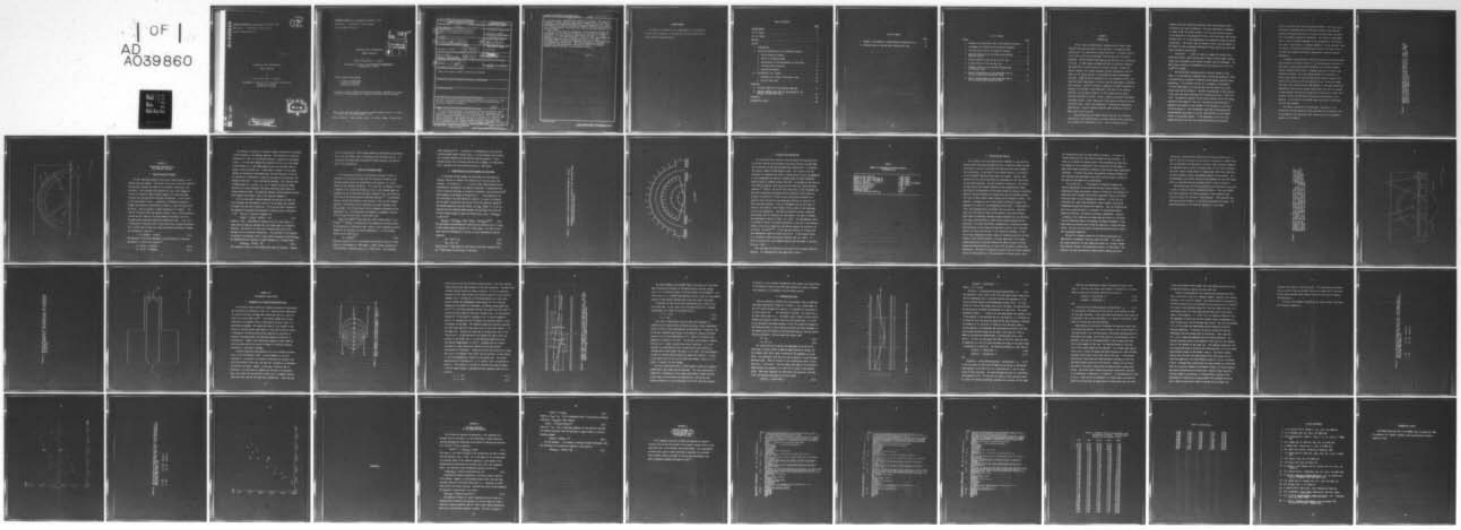

END

DATE
FILMED
6-77

TECHNICAL REPORT No. 13, series ii (February, 1977)

ONR Project: "Collisions of Ions in Gases"

Contract N00014-76-C-0127

(12) NW

A SPHERICAL PLATE ELECTROSTATIC ENERGY ANALYZER

by

José M. Perez and T. L. Bailey

Departments of Physics, and of Electrical Engineering
University of Florida
Gainesville, Florida

TECHNICAL REPORT No. 13, series ii (February, 1977)

ONR Project: "Collisions of Ions in Gases"

Contract N00014-76-C-0127

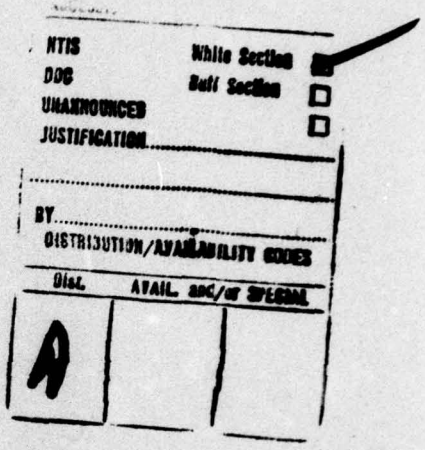

A SPHERICAL PLATE ELECTROSTATIC ENERGY ANALYZER*

by
José M. Perez** and T. L. Bailey

Departments of Physics, ~~and of Electrical Engineering~~
University of Florida

Project administered through:

College of Engineering
University of Florida
Gainesville, Florida

*This report was taken from the thesis of José M. Perez for the M. S. degree in Physics, Univ. of Florida (March, 1977)

**Present address: José M. Perez, 1610 S. W. 23rd St., Miami, Florida 33145

U

SECURITY CLASSIFICATION OF THIS PAGE (When Data Entered)

REPORT DOCUMENTATION PAGE

READ INSTRUCTIONS BEFORE COMPLETING FORM

1. REPORT NUMBER: Tech. Report No. 13, series ii
2. GOVT ACCESSION NO.: -----
3. RECIPIENT'S CATALOG NUMBER: ----------

4. TITLE (and Subtitle): (6) A SPHERICAL PLATE ELECTROSTATIC ENERGY ANALYZER.

5. TYPE OF REPORT & PERIOD COVERED: Scientific--Interim

6. PERFORMING ORG. REPORT NUMBER: ----------

7. AUTHOR(s): (10) José M. Perez and T. L. Bailey

8. CONTRACT OR GRANT NUMBER(s): (15) N00014-76-C-0127

9. PERFORMING ORGANIZATION NAME AND ADDRESS: Department of Physics (14) TR-13

10. PROGRAM ELEMENT, PROJECT, TASK AREA & WORK UNIT NUMBERS: NR 393-002

11. CONTROLLING OFFICE NAME AND ADDRESS: Physics Program, Office of Naval Research, Arlington, Virginia 22217 (12) 53 P.

12. REPORT DATE: (11) Feb[redacted]77

13. NUMBER OF PAGES

14. MONITORING AGENCY NAME & ADDRESS (if different from Controlling Office): (9) Technical rept.,

15. SECURITY CLASS. (of this report): U

15a. DECLASSIFICATION/DOWNGRADING SCHEDULE

16. DISTRIBUTION STATEMENT (of this Report)

Approved for public release; distribution unlimited

17. DISTRIBUTION STATEMENT (of the abstract entered in Block 20, if different from Report)

18. SUPPLEMENTARY NOTES

19. KEY WORDS (Continue on reverse side if necessary and identify by block number)

spherical electrostatic energy analyzer; variable-ratio electrostatic lens; ion-atom, ion-molecule collision experiments; kinetic energy spectrum; electronic, vibronic excitation.

20. ABSTRACT (Continue on reverse side if necessary and identify by block number)

A kinetic energy analyzer, to be used in proposed experimental studies of ion-atom and ion-molecule collision phenomena, has been designed and constructed. This instrument is of the electrostatic, 180° deflection type, and has hemispherical electrodes with radii of curvature of 1.400 and 1.600 inches respectively. The entrace and exit defining slits are identical circular apertures, 0.020 inches in diameter, spaced 3.000 inches apart. This configuration gives a nominal kinetic resolution of ~~±0.01E~~ +or- 0.01 E SUB 0, where E sub 0

DD FORM 1 JAN 73 1473 EDITION OF 1 NOV 65 IS OBSOLETE
S/N 0102-LF-014-6601

U 403 274

SECURITY CLASSIFICATION OF THIS PAGE (When Data Entered)

is the mean kinetic energy of ions entering the analyzer. The device is designed to operate with E_0 greater than or equal to 5 e.V, thus giving an optimum K.E. bandwidth for transmitted ions of $\Delta E_0 = \pm 0.05$ e.V. First-order aberrations, and the effects of fringing E fields in the vicinity of the defining apertures, have been taken into account quantitatively in the analyzer design.

One of the most important applications of the analyzer will be the measurements of K.E. spectra of energetic ions produced in 25-5000 e.V. collisions. For high resolution measurements (at $E_0 \geq 5$ e.V., giving $\Delta E_0 = 0.05$ e.V.), it is thus necessary to retard the fast ions leaving the collision region by a factor varying from about 5:1 to 1000:1. A relatively simple cylindrically-symmetric electrostatic lens system has been designed for this purpose. The rather extensive calculations necessary for this design were carried out by means of a computer program, based on paraxial ray electron-ion optics.

ACKNOWLEDGMENT

The authors are indebted to Mr. Ronald Spencer, of the Physics Research Shop, University of Florida, who did an excellent job of fabricating the energy analyzer.

TABLE OF CONTENTS

LIST OF TABLES

LIST OF FIGURES

CHAPTER I

INTRODUCTION

Several types of electrostatic charged-particle kinetic energy analyzers have been described in the literature. The parallel-ptate analyzer was first described by Yarnold and Bolton.[1] A further analysis of this device was given by Harrower,[2] who derived some of the basic equations. Eland and Danby[3] have used such an analyzer with a resolution of 25 meV. In 1929, Hughes and McMillen[4] built a cylindrical analyzer and showed that it could be used as an energy analyzer. Marmet and Kerwin[5] improved it by adding secondary electron suppression grids and used it as an energy selector, to give beams of nearly monoenergetic electrons. Rudd[6] derived an expression for its transmission curve, and Kuyatt and Rudd[7] proved that it could be used for measurement of absolute cross sections. Purcell[8] following a suggestion of Aston[9] introduced an analyzer with focusing in two dimensions in the form of the spherical capacitor; he also gave an analysis of the charged particle orbits, including relativistic effects. Hafner, Simpson, and Kuyatt[10] developed the theory further in their comparison of the spherical analyzer with the cylindrical type. Paolini and Theodoridis[11] obtained the transmission functions for a specific analyzer operated under conditions similar to those used in satellite work.

These devices have the common feature that ions (or electrons) traveling in a well-defined beam, but having different kinetic energies, are incident on an electrostatic field. Ions of different kinetic

energies then pass through the analyzing field along different paths, according to the laws of mechanics. The usual experimental arrangement is adjust either the kinetic energy of the ions entering the analyzer, or the magnitude of the analyzing $\vec{E}$ field, so that only those ions having energies which lie in the range $E_0 \pm \Delta E_0$ are transmitted through the device and detected. The various types of analyzers differ from one another in the shapes of their analyzing electrostatic fields, and of the electrodes used to establish these fields.

Electrostatic analyzers are used in a number of research areas, among these being: photo-electron spectroscopy, electron impact spectroscopy, mass spectrometry, and studies of atomic collision phenomena. The mean kinetic energies of transmitted ions vary from $E_0 \simeq 1$ eV or less to $E_0 \simeq 10^4$ eV or higher.

The electrostatic analyzer which is the main subject of this thesis is of the spherical condenser type, in which the analyzing $\vec{E}$ field is established by a potential difference placed between concentric metal hemispheres. Its principal use will be in ion-atom or ion-molecule collision experiments, to be carried out over the primary ion kinetic energy range 100 eV$<E_1<$5000 eV. The collision processes of most interest in this work are direct electronic (or vibronic) excitation: $A^+ + B = (A^+)^* + B^{**}$. The spherical analyzer will be used to measure the kinetic energy spectrum of the product A^+ ions, as a function of scattering angle Θ (measured with respect to the incident A^+ ion direction) as well as of collision energy E_1. Such information, when used in conjunction with energy-momentum conservation, provides identification of the internal states of the product species. If the experiments can be done with enough precision, they will also yield differential cross-sections

$\sigma(\Theta,E_1)$ for each of the various excitation channels. The latter would constitute a formidable body of information concerning the detailed nature of processes which occur in a given collision system, and would be of considerable theoretical importance. The success of experiments such as these is strongly dependent on the performance of the analyzer used, and in particular on its energy resolution. Of the available types of analyzer, the spherical condenser was chosen for this work since it not only gives adequate resolution, but possesses superior focusing properties.

A schematic cross-sectional view of the analyzer which was designed and constructed is shown in Figure 1. Its optimum energy resolution is $\Delta E_0 \simeq \pm 0.05$ eV, which should enable the device to distinguish between reaction channels which differ in internal energy by as little as one vibrational quantum. This high energy resolution is achieved in a fairly compact device by adjusting the kinetic energy of product ions entering the analyzer to the low value of $E_0 \simeq 5$ eV. Since the product ions leave their collision sites with energies in the range 100-5000 eV (depending on the collision energy), the product ions must be retarded in their passage from collision region to the analyzer by a large, and variable, factor, and then focused on the entrance aperture of the analyzer. A cylindrical electrostatic lens system which accomplishes this has been designed.

The theory of operation of the analyzer, the details of its fabrication, and the underlying theory and numerical calculations used in the design of the retardation lens system are given in subsequent sections of this thesis.

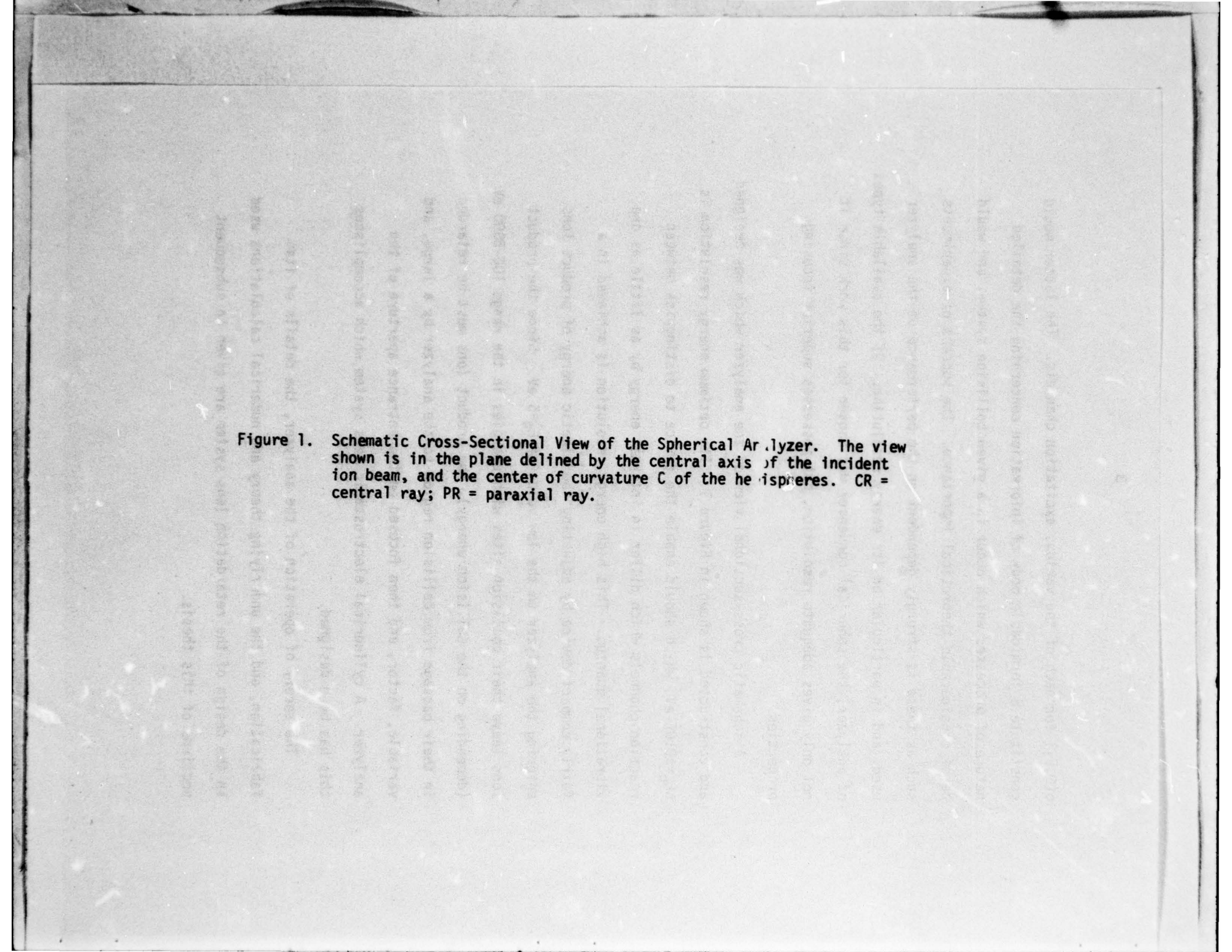

Figure 1. Schematic Cross-Sectional View of the Spherical Analyzer. The view shown is in the plane delined by the central axis of the incident ion beam, and the center of curvature C of the hemispheres. CR = central ray; PR = paraxial ray.

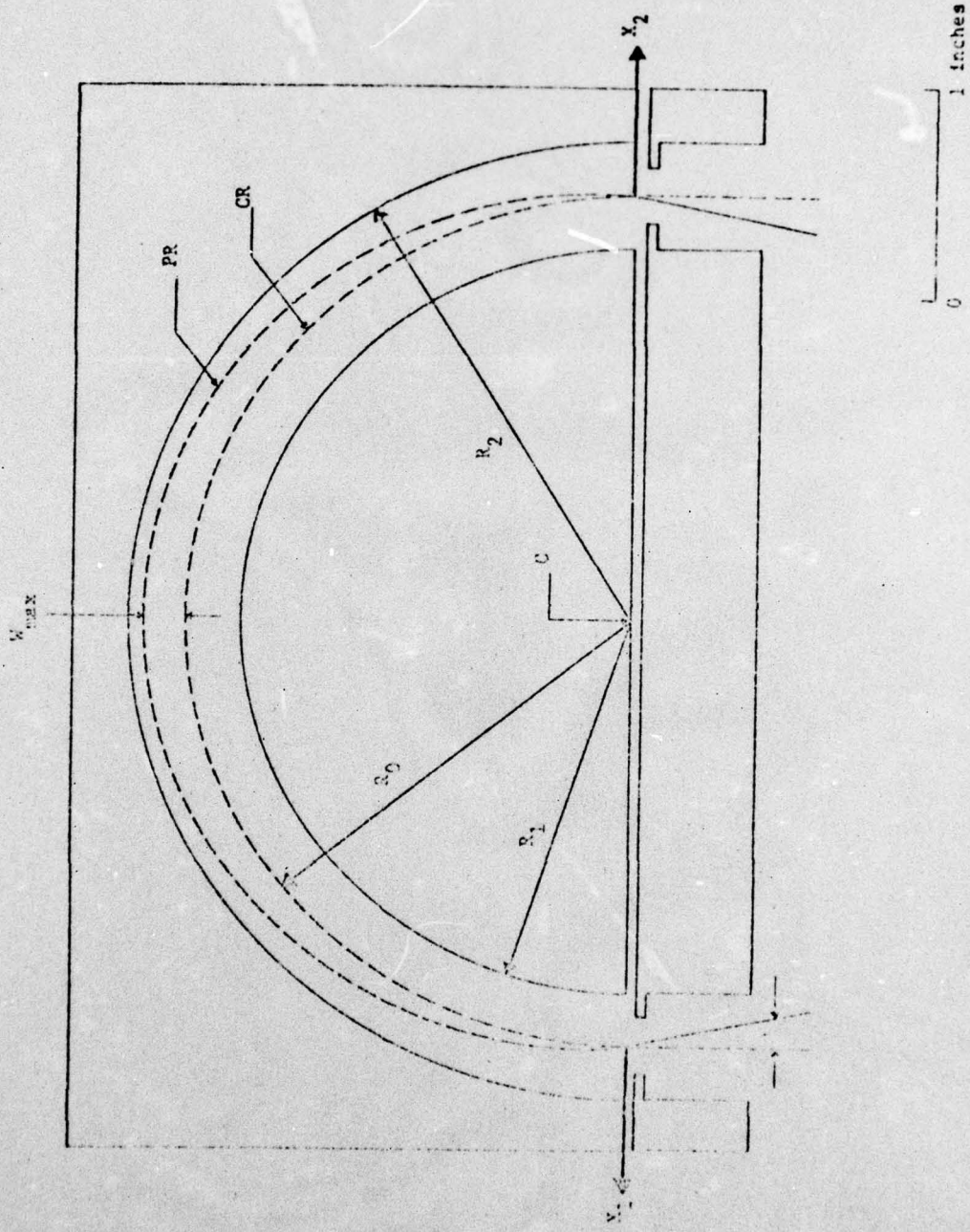
X_2
PR
CR
R_2
C
W_{max}
R_1
X_1
0
1 inches

CHAPTER II

DESIGN AND CONSTRUCTION OF THE SPHERICAL ANALYZER

1. Energy Dispersing Element

The most important element of any kinetic energy analyzer is the energy dispersing element. The choice in this work of the 180° spherical electrostatic analyzer was based on its property of focusing in two directions. This provides high transmission, and is well adapted to the use of relatively simple axially symmetric ion lenses for beam transport and focusing before and after the analyzer. In this device, a $1/r^2$ electrostatic field is produced by a difference of potential between two concentric hemispherical surfaces, of inner and outer radii R_1 and R_2. Such an analyzer is shown schematically in Figure 1. The ions (or electrons) enter the analyzer through a small circular aperture, located near the center of the space between the spheres, and leave (through another aperture) after being deflected by 180°. If $E_o = qV_o$ is the energy in electron volts of ions which travel through the analyzer on a circular path of radius R_o, then the potential difference V between the hemispheres is given by:

$$V = V_o [(R_2/R_1) - (R_1/R_2)] \tag{2.1}$$

The potential of the inner hemisphere, and the potential of the outer hemisphere, V_1, and V_2, are given by:[13]

$$V_1 = V_o [3 - 2 (R_o/R_1)] \tag{2.2}$$

$$V_2 = V_o [3 - 2 (R_o/R_2)] \tag{2.3}$$

The analyzer is required to transmit a beam of ions which is diverging in two directions at the entrance aperture. The direction of a given ion trajectory (or "ray") at the entrance aperture is specified by the angles α and β. α is the angle between the projection of this ray on the plane of the analyzer (i.e., the plane shown in the cross-sectional view of Figure 1) and the central ray. β (not shown in Figure 1) is the angle between the direction of the central ray, and the projection of the ray of interest on a plane which is normal to the plane of the analyzer, and tangent to the central ray at the entrance aperture. The limiting values of these angles are $\pm \alpha_m$ and $\pm \beta_m$. In the equation giving the image position in an actual analyzer, the terms containing these angles are called aberration terms. The spherical analyzer provides perfect focusing with respect to the angle β, due to its spherical symmetry.[8]

Let X_1 be the radial distance measured from the path of radius R_o of an incident ion with energy E, and let α be the angle this incident ion makes with the path of radius R_o. Let X_2 be the radial distance of the outgoing ion measured from the path of radius R_o after a deflection of 180°. Then (as is derived in Appendix A)

$$(X_2/R_o) + (X_1/R_o) = 2(\Delta E/E_o) - 2\alpha^2 \qquad (2.4)$$

where $\Delta E = E - E_o$. The absence in equation (2.4) of a term linear in α shows that the spherical analyzer has first order angle (or direction) focusing. The values of X_1 and X_2 are limited by the sizes of the entrance and exit apertures respectively. The resolution of the analyzer is defined as the maximum value of $\Delta E/E_o$ given by equation (2.4), $(\Delta E/E_o)_{max}$. For entrance and exit apertures of equal diameters W, it follows that:

$$(\Delta E/E_o)_{max} = (W/2R_o) + \alpha_m^2 \qquad (2.5)$$

This equation is basic for the design of the spherical analyzer. However,

it is no longer valid if the distance between the hemispherical electrodes, ΔR, is not sufficiently small in comparison with the mean radius R_o. In such cases the second-order aberrations[12] become important, and must be taken into consideration.

2. Choice of Acceptance Angle

The transmission function of the spherical analyzer, $T(E;V_o)$ is defined as the fraction of those ions (or electrons) incident on the entrance aperture which are transmitted by the analyzer, at a given setting of the analyzer voltage V_o. For a given V_o, the shape of T versus E depends on the current distribution of ions in the incident beam, the maximum size of the aberration term α_m^2 in equation (2.5), and finally on the sizes of the entrance and exit defining apertures.[11] In the present design a uniform distribution of the current of ions over the entrance aperture, and entrance and exit apertures with equal diameters, have been assumed. The $T(E;V_o)$ versus E profile depends considerably on the magnitude of α_m. This aberration term produces an asymmetric tailing of the $T(E,V_o)$ versus E curve, on the high-E side.

Kuyatt and Simpson[13] found that this effect becomes small if $\alpha_m \leq (W/2R_o)^{1/2}$. However, a correction of the transmission function profile by decreasing α_m to arbitrarily small values is not an adequate solution, because of the intensity loss which accompanies it. In the present design, α_m was chosen to be

$$\alpha_m = (W/4R_o)^{1/2} \tag{2.6}$$

then when equation (2.6) is substituted into equation (2.5), with a mean radius for the spheres of 1.500 inches, a kinetic energy resolution of 1/100 requires an aperture width of W = 0.020 inches. The acceptance

angle becomes $\alpha_m \simeq 3.13°$. To provide a collimated beam of ions with the desired maximum spread in angle ($\pm\alpha_m$), a circular aperture can be placed at a suitable distance from the defining entrance aperture. In the present design, this collimating aperture has a diameter of 0.089 inches and is separated from the entrance aperture by 1.000 inches.

3. Determination of the Gap Between the Electrodes

To determine the gap between the electrodes ΔR of the spherical analyzer, one has to consider the trajectories of the ions within the analyzer. In a central force field (such as that formed between the two hemispherical electrodes of the spherical analyzer), a charged particle (ion or electron) describes an elliptical trajectory, with an eccentricity[11] which depends on the energy of the particle E. The trajectory of an ion with energy E has been obtained in terms of its point of incidence and its angle α relative to the central ray of the spherical analyzer[12]. The maximum separation from the central ray, W_{max} (Figure 1), of an ion entering into the analyzer midway between the electrodes and having the maximum allowed spreads in angle and energy ($\alpha=\alpha_m$, $\Delta E/E_o = (\Delta E/E_o)_{max}$), is given by[13]

$$(W_{max}/R_o) = (\Delta E/E_o)_{max} + [\alpha_m^2 + (W/2R_o + (\Delta E/E_o)_{max})^2]^{1/2} \qquad (2.7)$$

The gap between the hemispherical electrodes was chosen to be $\Delta R = 2\ W_{max}$. In the present spherical analyzer $\Delta R = 0.200$ inches. The radii of the inner and outer hemispheres, R_1 and R_2, are thus determined by the two equations:

$$(R_1 + R_2)/2 = R_o \qquad (2.8)$$

$$(R_2 - R_1) = \Delta R \qquad (2.9)$$

These give $R_1 = 1.400$ inches for the radius of the inner hemisphere and $R_2 = 1.600$ inches for the radius of the outer.

Figure 2. Arrangement of Fringing Field Shielding Diaphragms S_1, and S_2.[a]

([a]Proposed by Wollmick for the correction of the fringing $\bar{E}$-field, in toroidal-type energy analyzer.)

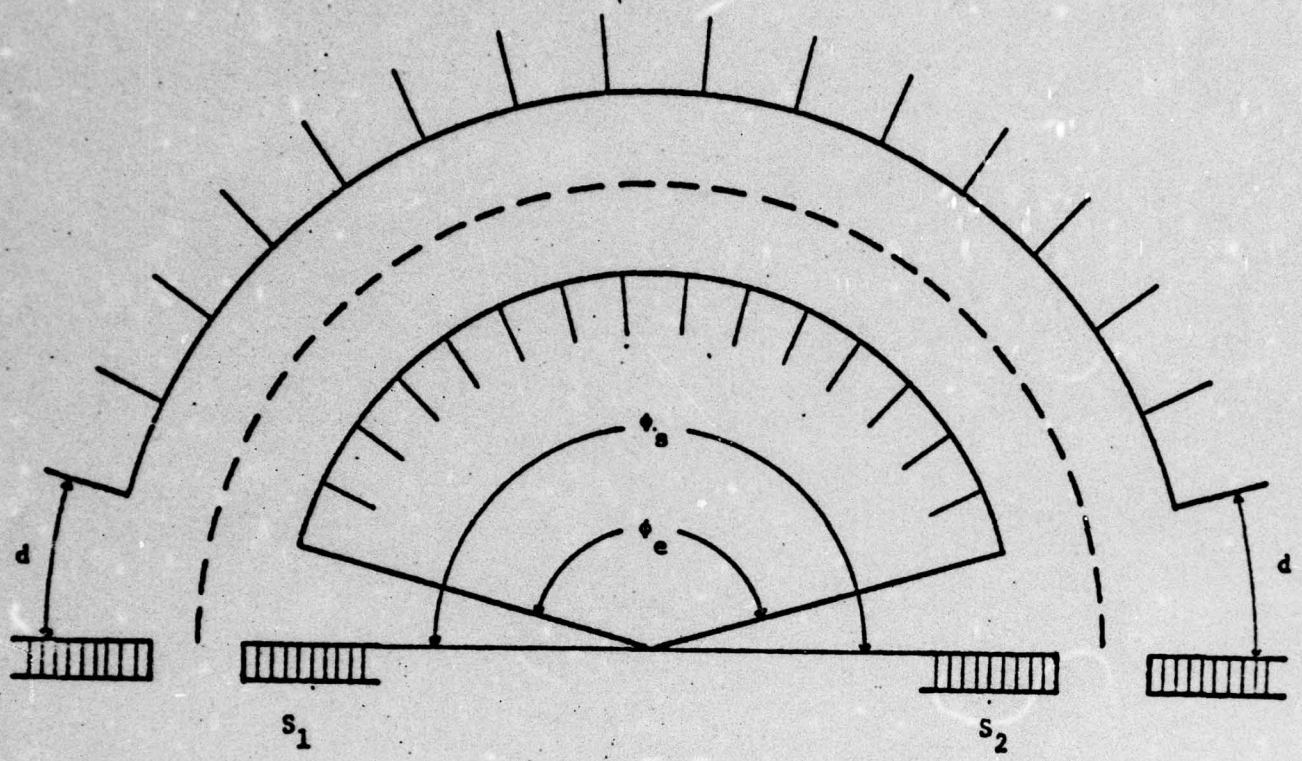

$$\phi_s = \phi_e + 2d$$

4. Fringing Field Corrections

The fringing $\vec{E}$-field outside of the gap between the hemispheres has so far been ignored, and calculations have been performed assuming that the trajectories of the ions are those which would prevail in completely rotationally symmetric electrostatic fields. The fringing field has the effect of increasing the angle Φ_s through which the ions are deflected, so that a hemispherical analyzer (Φ_e=180°) gives an actual deflection angle Φ_s which is somewhat greater than 180°. An estimate of the required correction was made by using the correction factor for a parallel plate condenser.[14] Wollnik and Ewald[15] have shown that, if the electrodes and the plane containing the entrance and exit apertures of the spherical analyzer are placed as in Figure 2, the calculations performed for a parallel plate analyzer are also good approximations for spherical (or other toroidal) analyzers. With an arrangement such as that shown in Figure 2, the effects of the fringing fields outside of the diaphragms S_1 and S_2 are negligible. The angle Φ_s between the planes containing the entrance and exit apertures (or equivalently, the angle Φ_s between the diaphragms S_1 and S_2) is then: $\Phi_s = \Phi_e+2d$. The supplementary angle d, defined in Figure 2, has been calculated as a function of the aperture width W, the principal radius R_0, and the gap between the electrodes ΔR, by Wollnik and Ewald[12,15]. In the spherical analyzer of interest here the supplementary angle was found to be d≃1.8°. In the present design it is desirable to have focusing at precisely 180° (Φ_s = 180°). In order to achieve this, the azimuthal angle of the electrodes is required to be Φ_e = 176.4°.

This concludes the discussion of the design of the present spherical analyzer. Its characteristics are summarized in Table 1.

Table 1.

Summary of the Spherical Energy Analyzer Characteristics

Analyzer mean radius R_0	1.500 inches
Radius of the inner electrode R_1	1.400 inches
Radius of the outer electrode R_2	1.600 inches
Effective entrance aperture W	0.020 inches in diameter
Effective exit slitwidth	0.020 inches
Energy in deflector E_0	5 eV
Energy resolution ΔE	0.05 eV
Acceptance angle α	3.13°
Electrode deflection angle Φ_e	176.4°

5. Constructional Details

The validity of the calculated design parameters for the spherical analyzer which have been presented thus far is doubtless subject to some restrictions, because of the idealized conditions which were assumed in the calculations. As set forth in the previous Section 4, the effects of the fringing $\vec{E}$ field have been taken into account. However, other perturbing factors which can affect the performance of this device have (so far) been neglected. The most important of these are: the effects of space-charge (or Coulomb) spreading of the charged-particle beam; the effects of contamination of electrode surfaces by layers of insulating material; and the reflection of charged particles by electrode surfaces. The first of these factors (space charge) can be disposed of easily. This analyzer is designed for use in the product-ion analyzer system of an apparatus for studies of ion-atom/molecule collisions. In these applications, the estimated fluxes of product ions are very low: typically, only a few ions would be found in the analyzer at any given instant. Under these circumstances the mean distances between ions are relatively very large, and the effects of their mutual Coulomb interactions are negligible. The other two effects (contamination of electrode surfaces, and reflection of ions) cannot be dismissed so easily, but it has been possible to design the analyzer so that these are minimized. In the case of the contamination effect, layers of insulating material (arising primarily from diffusion pump oil, or other impurities in the vacuum system) deposited on electrode surfaces can acquire volume or surface charge distributions which can, in turn, alter the paths of nearby ions drastically. The effect is especially serious if the ion kinetic energies are low (as they would be, in the experiments of interest here), and if

the contamination occurs on small defining apertures. It results in reduced transmission of ions, and in unsteady ion beam currents. Its cures are to design the vacuum system so that background gas impurities are reduced as far as practicable, and to fabricate the electrodes of metal which tends to maintain a relatively clean surface under experimental conditions. To achieve the latter, the spherical analyzer entrance and exit apertures have been made of pure gold, and the interior surfaces of the analyzer electrodes will be gold-plated.

For a given setting of the potential difference V between the analyzer hemispheres we have seen that the mean kinetic energy of ions transmitted through the analyzer, $E_o=qVo$, is related to V by Equation (1). Ions with kinetic energies which differ appreciably from E_o will strike either the inner or outer hemispherical surfaces. If such ions are reflected from, rather than absorbed by, these surfaces, they can be transmitted through the analyzer exit aperture. Thus ion reflection can give rise to spurious peaks, or structure, in the measured kinetic energy distributions, and these are obviously undesirable. Previous experience in this laboratory has shown that the effects of ion reflection are diminished greatly, and perhaps eliminated altogether, if the inner electrode surfaces have a matte (as opposed to a highly polished) finish. The gold (or gold plate) surfaces mentioned previously satisfy this requirement adequately.

The metallic elements (except for the defining apertures) are fabricated of non-magnetic stainless steel (S/S 304). This material was chosen because of its high dimensional stability, relative freedom from internal stresses, and satisfactory behavior in high vacuum. The spherical surfaces were machined using the OD-ID combination radius

turning tool, manufactured by Ralmikes Tool-A-Rama Corporation (cat. # 006-14), giving an accuracy for the radius of curvature of ±0.0005 inches. The two hemispheres are mounted on a stainless steel baseplate (Figure 3) and separated from it by KEL-F insulator disks of 1/16 inches thickness. Three KEL-F dowels (0.250 inches in diameter and 0.960 inches long) give precise alignment of the two hemispheres relative to one another. The two hemispheres are rigidly attached to the baseplate by four 6X32 screws, which are insulated from the baseplate by KEL-F sleeves (Figure 3).

The entrance and exit defining apertures are fabricated of pure gold, in order to minimize surface contamination effects. These are mounted with their respective collimating apertures in two removable plugs (Figure 4) which fit into holes in the baseplate. These apertures have been machined with chamfers, so that they approximate knife edges. The approximate weight of the spherical analyzer is 16.25 pounds.

Figure 3. Cross-Sectional View of the Spherical Analyzer. The inner and outer hemispheres (the curved surfaces of parts A and C respectively) are mounted on a baseplate (part B). Disks and sleeves constructed of KEL-F (parts I) provide the necessary insulation between the metallic parts A, B, and C. Defining apertures and colliminating apertures are constructed in two removable plugs (parts P) and mounted on the baseplate. Dowels (Part D) provide precise alignment.

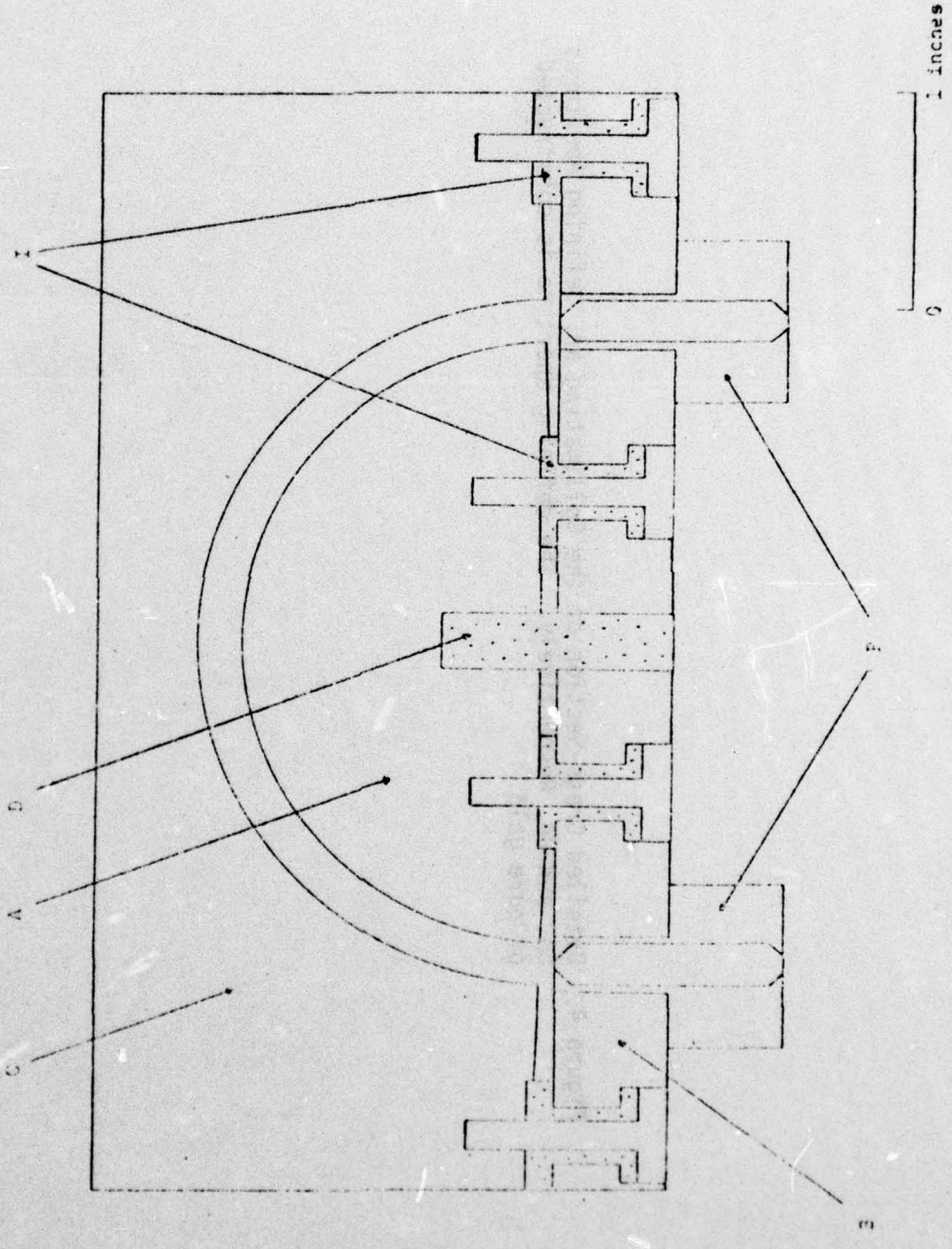
1 inches
0
H
B
A
C
E
S

Figure 4. Detailed Cross-Section of the Collimating and Defining Apertures CA, and DA, Respectively. The defining aperture is constructed of pure gold.

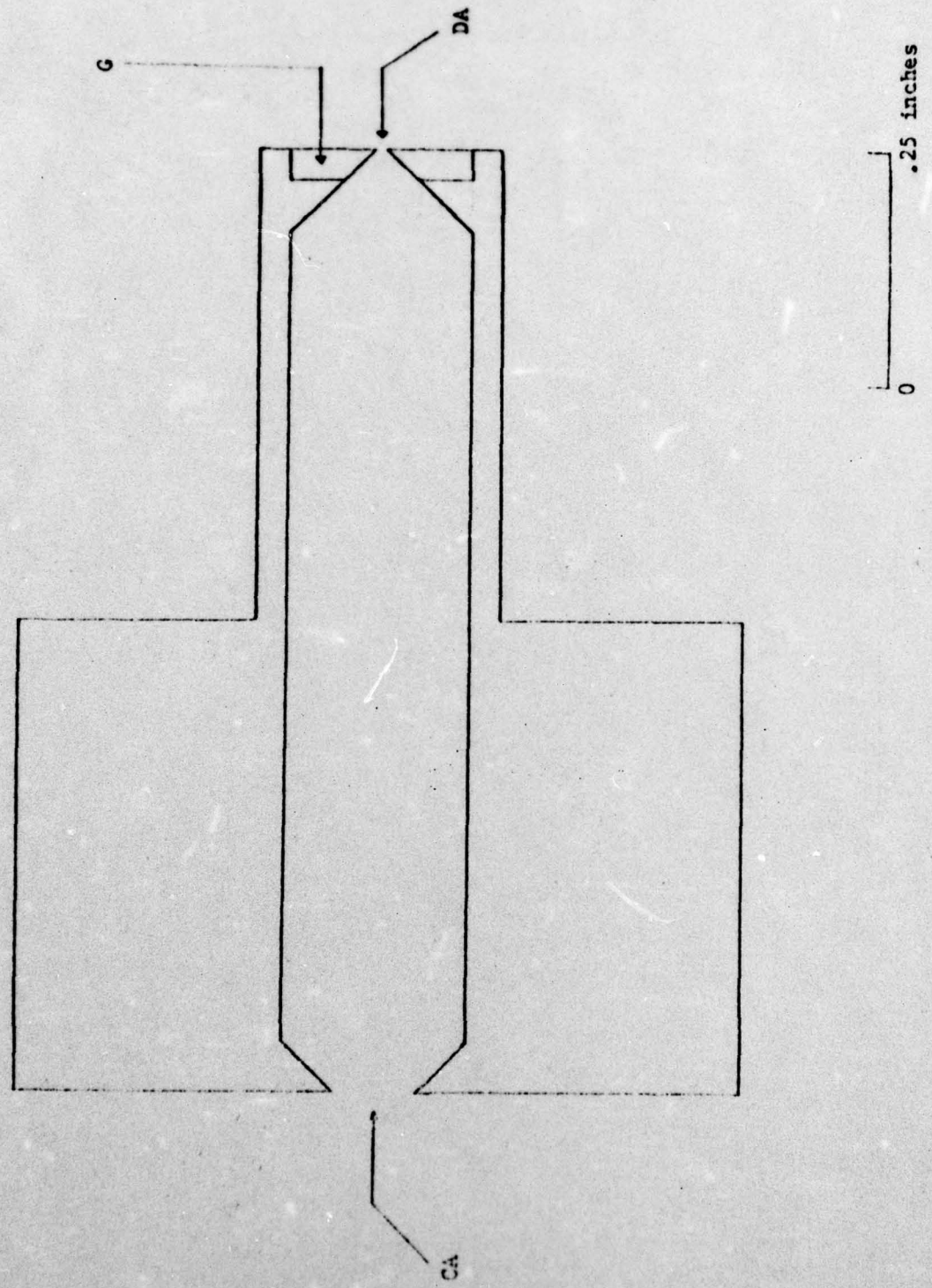
G
DA
CA
0
.25 inches

CHAPTER III

ELECTROSTATIC LENS SYSTEM

1. Parameters of a Single Electrostatic Lens

Electrostatic fields with axial symmetry accelerate (or decelerate) and focus paraxial electrons or ions (i.e., those particles whose paths lie close to the axis, and make small angles with the axis) much as a glass lens focuses light rays[16]. If an axially symmetrical or a two-dimensional electrostatic field is specified on the axis, then it is determined everywhere. This means that there is less freedom in the design of electrons lenses than there is in the case of optical lenses. A knowledge of the electrostatic field along the axis provides all necessary information about the focusing properties of the lens in consideration. Figure 5 shows the axially symmetric field formed by applying potentials to two coaxial cylinders of different diameters, separated by a small gap in between.

Evidently other electrode geometries will give different distributions of the electrostatic field. From the geometry of the lens electrodes it is possible in principle to determine the potential and field distribution in the lens, and from this information, to determine all possible ion paths. However, in the case of paraxial ions or electrons, it is sufficient to compute only the path of two paraxial rays, which enter the lens parallel to the Z-axis of symmetry from the right hand side, and the left hand side, respectively. These two rays

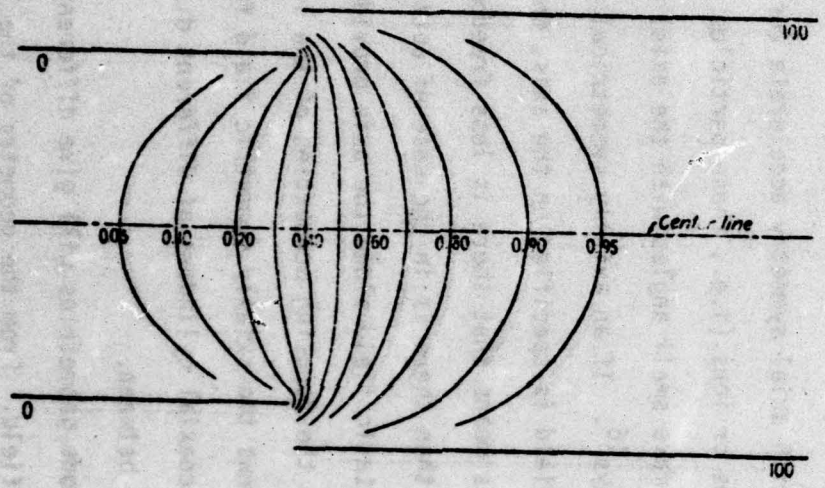

Figure 5. Axially Symmetric Field Formed by Applying Potentials to Two Coaxial Cylinders of Different Diameters. $D_2/D_1=1.5$.

can be used to give the so-called "cardinal points" of the lens, and the latter describe the image formation of the lens completely. The definitions of these cardinal points are shown in Figure 6. An ion (or electron) entering the lens from the left, and initially parallel to the Z-axis of symmetry (ray 1' in Figure 6), is deflected towards the Z-axis while passing through the inhomogeneous electrostatic $\bar{E}$-field in the gap between the two cylindrical electrodes, and emerges headed toward the axis.[18] At sufficient distances from the lens region the ions travel in field-free space, and their paths are straight lines. The intersection between the initial parallel trajectory (ray 1') and the asymptotic path of the emerging ion (ray 2') defines the principal plane H', which corresponds to the image. The distance between the principal plane and the point where the ion crosses the Z-axis, is the "focal length" f' of the image side. The point at which the ion crosses the Z-axis is the "focal point." In the same way an ion coming from right to left and parallel to the Z-axis (ray 1) is also deflected toward the Z-axis, and emerges headed towards it (ray 2). Extending the two straight trajectories, their intersection defines the principal plane H corresponding to the object. The point at which the emerging ion crosses the Z-axis is the object "focal point" and its distance f to the plane H is the corresponding focal length f of the object side. The lateral magnification M is defined as $M = -Y'/Y$, where Y' and Y are defined in Figure 6. From Figure 6 it can also be seen that the object distance P and the image distance Q, measured from the reference plane Z=0, are given by:

$$P = F + f/M \tag{3.1}$$

$$Q = F' + f'M \tag{3.2}$$

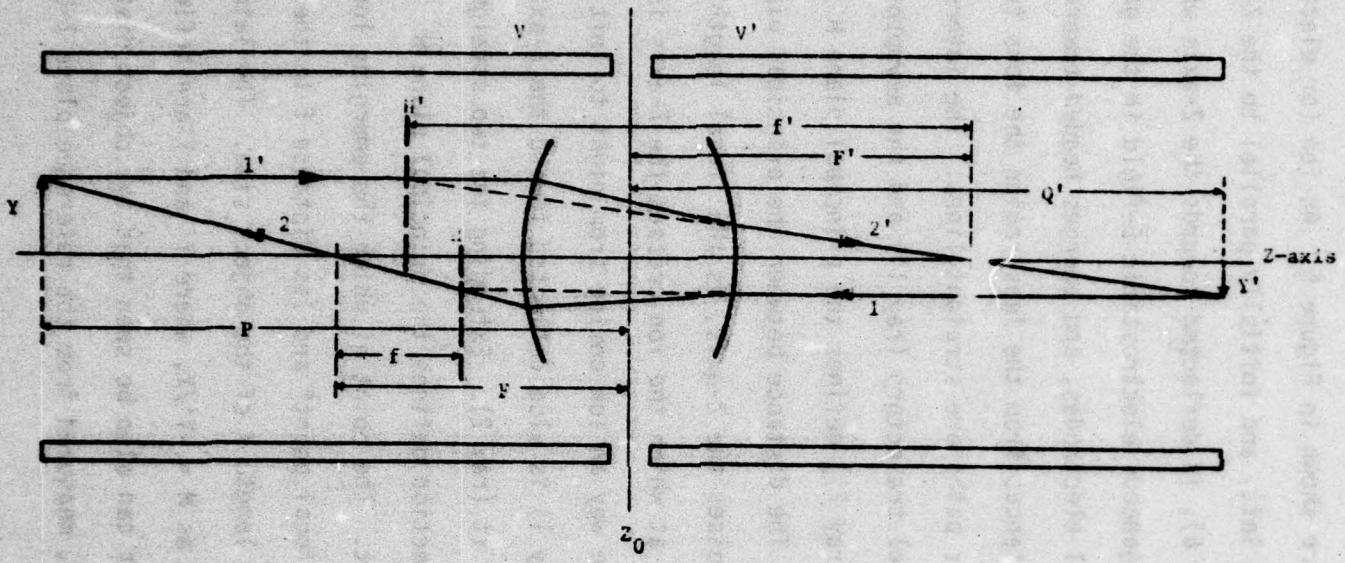

Figure 6. Cardinal Points Corresponding to a Two-Tube Electrostatic Lens. The focal lengths F and F', as well as the positions of the principal planes H and H', depend on the voltage ratio between the two electrodes V/V'.

For equal-diameter, two-cylinder lenses, the values of P and Q have been calculated as functions of the magnification M and the voltage ratio V'/V for different values of the gap between the electrodes[16]. In a recent work, A. B. El-Kareh[17] has obtained accurate values for the cardinal points of lenses having voltage ratios within the range $1.5 \leq V'/V \leq 50$.

If desired the lens can be used to decelerate ions, as well as to accelerate them. In this case, V'<V; the magnification M is inverted, and equations (3.1) and (3.2) are then given by:

$$P = F' + f'/M \tag{3.3}$$

$$Q = F + fM \tag{3.4}$$

This kind of electrostatic lens has been used frequently in accelerating (or decelerating) and focusing systems in many experimental devices in which a fixed acceleration (or deceleration) is required. One of the most important applications of the spherical analyzer described previously will be the measurements of K.E. spectra of energetic ions produced in 25-5000 eV collisions. The analyzer was designed to operate with $E_0 \simeq 5$ eV, in order to obtain high energy resolution. It is thus necessary to retard the fast ions leaving the collision region by a variable factor which ranges from about 5:1 to 1000:1, and simultaneously to keep the distance between object and image (P+Q) constant. A single (2-cylinder) lens will not satisfy these requirements, since as V'/V is varied, in general P+Q also changes.

For the present application, a three-element cylindrically-symmetric electrostatic lens system has been designed. This lens system (which is essentially a combination of two single electrostatic lenses) provides a wide range of accelerations and decelerations, and has the same focusing properties of any electrostatic field with rotational symmetry.

An analysis of this variable voltage-ratio lens system, and a description of the numerical results which have been obtained for several different lens geometries, are presented in the following section.

2. Variable Ratio Lens

One can construct a variable ratio electrostatic lens by combining two single electrostatic lenses as in Figure 7. For a large number of pairs of values assigned to V_1 and V_2, it is possible to find values of V_F which satisfy the focusing condition of the lens. For simplicity L_1 has been chosen equal to L_3. The length $L_2 > 2D$ in order to avoid overlap between the potential fields of the first and second stage. If P_1 and Q_1 are the object and image distances of the first stage with respect to the reference plane Z_1, and P_2 and Q_2 the object and image distances of the second stage with respect to the reference plane Z_2, then the overall focusing conditions of the two stage lens require that:

$$P_1 = Q_2 \tag{3.5}$$

$$Q_1 + P_2 = L_2 \tag{3.6}$$

For fixed values of P_1 and Q_2, the magnitudes of Q_1 and P_2 are determined in terms of their respective magnifications M_1 and M_2, and the voltage ratios V_F/V_1, V_2/V_F, according to the equations (3.1) and (3.2). The conditions (3.5) and (3.6) can be applied to three different operating modes. Mode A-A consists of two accelerating stages; in this case $V_F/V_1 > 1$. and $V_2/V_F > 1$. Then the object and image of an accelerating stage are given by equations (3.1) and (3.2) in terms of the cardinal points. When these equations are substituted into equations (3.5) and (3.6), the focusing conditions of the lens become

$$F_1(V_F/V_1) + f_1(V_F/V_1)/M_1 = L \tag{3.7}$$

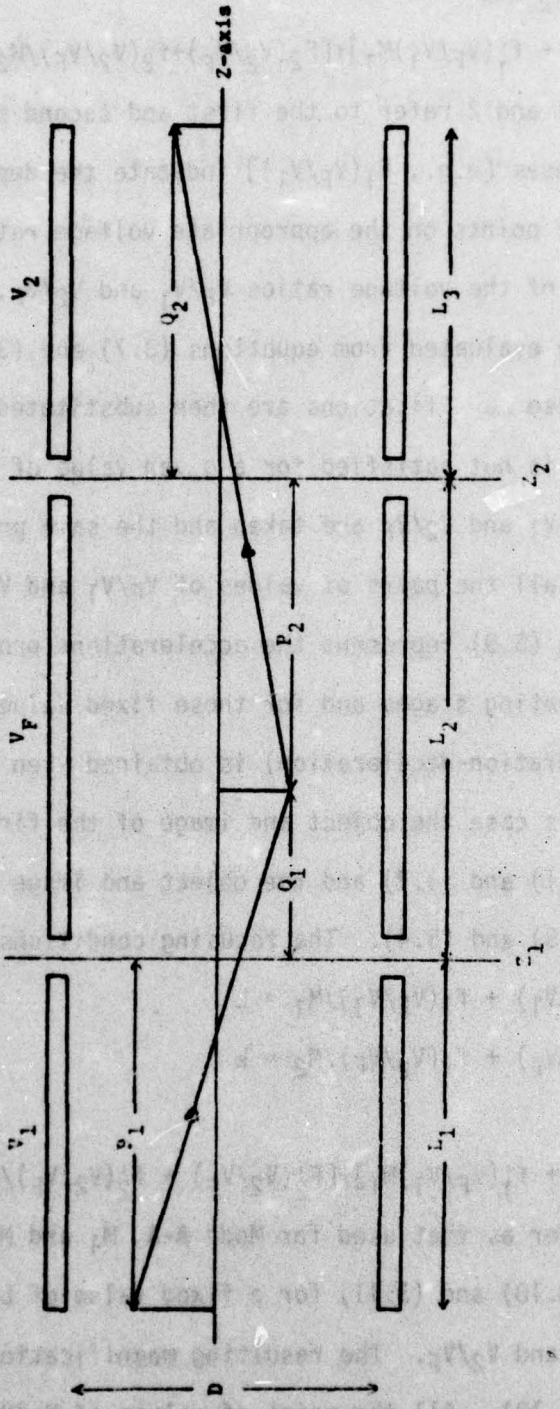

Figure 7. Schematic Drawing of a Variable Voltage Ratio Electrostatic Lens.

$$F_2'(V_2/V_F) + f_2'(V_2/V_F)M_2 = L \tag{3.8}$$

where $L = P_1 = Q_2$ and

$$[F_1'(V_F/V_1) + f_1'(V_F/V_1)M_1]+[F_2(V_2/V_F)+f_2(V_2/V_F)/M_2] = L_2 \tag{3.9}$$

The subscripts 1 and 2 refer to the first and second stages respectively, and the parentheses [e.g., $F_1(V_F/V_1)$] indicate the dependences of the various cardinal points on the appropriate voltage ratios. For given values of L and of the voltage ratios V_F/V_1 and V_2/V_F, the magnifications M_1 and M_2 can be evaluated from equations (3.7) and (3.8). The values obtained for these magnifications are then substituted into equation (3.9). If the equation is not satisfied for a given value of L_2, a different set of values of V_F/V_1 and V_2/V_F are taken and the same procedure is repeated. The products of all the pairs of values of V_F/V_1 and V_2/V_F found to satisfy equation (3.9) represent the accelerations provided by the lens with two accelerating stages and for those fixed values of L and L_2.

Mode A-D (acceleration-deceleration) is obtained when $V_F/V_1>1$ and $V_2/V_1<1$. In this case the object and image of the first stage are given by equations (3.1) and (3.2) and the object and image of the second stage by equations (3.3) and (3.4). The focusing conditions are then given by

$$F_1(V_F/V_1) + f_1(V_F/V_1)/M_1 = L \tag{3.10}$$

$$F_2(V_2/V_F) + f_2(V_2/V_F)/M_2 = L \tag{3.11}$$

and

$$[F_1'(V_F/V_1) + f_1'(V_F/V_1)M_1]+[F_2'(V_2/V_F) + f_2'(V_2/V_F)/M_2] = L_2 \tag{3.12}$$

In the same manner as that used for Mode A-A, M_1 and M_2 are determined from equation (3.10) and (3.11) for a fixed value of L, and for given values of V_F/V_1 and V_2/V_F. The resulting magnifications are substituted into equation (3.12). All the pairs of values of V_F/V_1 and V_2/V_F found to satisfy the focusing conditions represent the solutions for this mode.

Mode D-D (two deceleration stages) corresponds to $V_F/V_1<1$ and $V_2/V_F<1$. Obviously this mode is the inverse of the Mode A-A. For this mode of operation the focusing conditions are given by

$$F_1'(V_F/V_1) + f_1'(V_F/V_1)/M_1 = L \tag{3.13}$$

$$F_2(V_2/V_F) + f_2(V_2/V_F)M_2 = L \tag{3.14}$$

and

$$[F_1(V_F/V_1)+f_1(V_F/V_1)M_1]+[F_2'(V_2/V_F)+f_2'(V_2/V_F)/M_2] = L_2 \tag{3.15}$$

The calculations for Mode D-D are carried out in the same way as those for the other two modes. Since the present electrostatic lens system can be operated in any of the three modes, it is capable of providing a wide range of accelerations and decelerations.

When dealing with practical instruments two important factors have to be taken into account. The first of these is the "filling factor" of the electrostatic lens, and the second is the maximum deceleration ratio permitted in one stage. The filling factor of an electrostatic lens is defined as the ratio of the maximum width of the ion beam within the lens to the diameter of the lens. For good performance of the lens, this filling factor should be less than 50%. In a single stage electrostatic lens, in which the object and image distances are fixed, defining apertures can be used to limit the width of the beam. In the present electrostatic lens system the image and object distances of the first and second stages respectively are variable. However, we can control the width of the beam by restricting the magnifications to have small values. The second factor affects the present electrostatic lens when it is operated as in Mode A-D, or in Mode D-D. A large deceleration ratio as (e.g., 1:100) can not be tolerated in a single stage, since the lens would be so strong that the image would be formed inside the lens field.

In the calculations of the present lens, the maximum deceleration ratio allowed per stage was chosen to be less than 1:50.

Extensive calculations of this variable-ratio electrostatic lens were carried out by means of a computer program. Basically this program executes a trial and error method. The cardinal points corresponding to different voltage ratios (as obtained from the calculations of El-Kareh[17]) are stored in two identical arrays (Xi), and (Xj), where the array (Xi) correspond to the first lens stage and the array (Xj) to the second stage. Every element of each array (Xi) is a vector of dimension five, the components of which are the four cardinal points corresponding to a given voltage ratio, and the voltage ratio itself. The first two elements (i=1, j=1) are taken and substituted into the equations giving the focusing conditions. If the pair (X_1 and X_1) satisfy the focusing conditions, then the voltage ratio is printed out. Then a new pair (i=1, j=2) is taken and compared with the focusing conditions. The process terminates when all the elements of the array (Xi) are compared with all the elements of the array (Xj). This computer program was used to calculate the range of accelerations (decelerations) of various lenses with different values of the lengths L and L_2. The overall voltage ratio of the lens V_2/V_1 has been plotted versus the voltage ratio of the first stage V_F/V_1, for two different values of L and L_2, in Figures 8 and 9. Although these calculations have been confined to a three-tube lens of a particular geometry (equidiameter lenses), one could obviously do similar calculations with electrostatic lenses of other geometries. The wide range of accelerations (or decelerations) required in the experiments of interest here ($5 \leq V_2/V_1 \leq 1000$) can be accomplished using two of these variable ratio lenses in cascade (as for example two

variable ratio lenses of L=3D and L_2=3D). This combination also permits the use of one of the two variable lenses as an Einzel lens[17] (for which $V_1=V_2$), which provides great range of control of the focus by varying the potential V_F.

Listings of the computer programs and the input cardinal point data, are included in Appendix B.

Figure 8. Plot of the Overall Voltage Ratio V_2/V_1 Versu the Voltage Ratio of the First Stage V_F/V_1 of the Three-Tube Lens, at the High Acceleration Operational Mode (Mode A-A).

L = 3D L_2 = 4D (curve 1)

L = 3D L_2 = 3D (curve 2)

V_F/V_1
0.00
10.00
20.00
30.00
40.00
50.00
V_2/V_1
0.00
15.00
30.00
45.00
60.00
75.00
(X10¹)
(1)
(2)

Figure 9. Plot of the Overall Voltage Ratio V_2/V_1 Versus the Voltage Ratio of the First Stage V_E/V_1 of the Three-Tube Lens, at the Low Acceleration Operational Mode (Mode A-D).

$L = 3D$ $L_2 = 4D$ (curve 1)

$L = 3D$ $L_2 = 3D$ (curve 2)

V_2/V_1
5.00
4.00
3.00
2.00
1.00
0.00
V_F/V_1
50.00
40.00
30.00
20.00
10.00
0.00
(1)
(2)

APPENDICES

APPENDIX A

THE BASIC EQUATION OF THE SPHERICAL ANALYZER

The differential equation corresponding to the trajectory of a charged particle of energy E, in the electrostatic field produced by the two hemispherical electrodes of the spherical analyzer was obtained by H. Wollnik [12] and is given by:

$$d^2u/d\Phi^2 + u = E_oR_o/R_{\Phi=0}\ E\cos^2\alpha \qquad (A.1)$$

where $R_{\Phi=0}$ is the radial distance of the charged particle when it enters into the analyzer, and $u = R_o/R$. R_o is the radius of the circular path (or principal path) of the spherical analyzer, E_o the energy of the charged particle describing the principal path, and α the acceptance angle. The solution of the differential equation has the form:

$$u=(R_oE_o/R_{\Phi=0}\ E\cos^2\alpha)(1-\cos\Phi)+\cos\Phi-\tan\alpha\sin\Phi \qquad (A.2)$$

Expanding the factors containing α, we find all powers from the first present. However, at the azimuthal angle $\Phi=180°$, the last term vanishes, and with it the only linear term in α. Therefore at $\Phi=180°$ there exists first-order focusing. Choosing that value of Φ and expanding the equation to second order in α, we have

$$R_o/R_{\Phi=180} = (2E_oR_o/E\ R_{\Phi=0})(1+\alpha^2)-1 \qquad (A.3)$$

The spherical analyzer is usually operated with V=0 at $R=R_o$ so a charged particle entering the analyzer at a value of $R\neq R_o$ will enter a region at a nonzero potential and will lose or gain energy depending on what part of the defining aperture it enters. The loss of energy is

$$qV(X_1) = 2\,E_0X_1/R_0 \qquad (A.4)$$

where $X_1 = R_{\Phi=0} - R_0$. This is subtracted from E in the previous equation. Letting $X_2 = R_{\Phi=180}-R_0$, there results:

$$X_2/2R_0 = -(X_1/2R_0)+(\Delta E/E_0)-\alpha^2 \qquad (A.5)$$

where $\Delta E = E-E_0$. This is the basic equation for the spherical analyzer. For defining entrance, and exit apertures of equal widths W, the basic equation becomes

$$(\Delta E/E_0) = (W/2R_0) + \alpha^2 \qquad (A.6)$$

For the maximum allowed spreads in energy and angle ($(\Delta E/E_0)max$, α_m^2), the resolution of the spherical analyzer is then given by

$$(\Delta E/E_0)_{max} = (W/2R_0) + \alpha_m^2 \qquad (A.7)$$

APPENDIX B

COMPUTER PROGRAMS USED IN THE CALCULATIONS OF THE VARIABLE VOLTAGE RATIO ELECTROSTATIC LENS

In this Appendix have been included and detailed the computer programs used for the calculations of the overall voltage ratios of the three-tube lens in the different operational modes. The corresponding cardinal points used in these calculations have been also included. These cardinal points correspond to the two-tube equidiameter lens, with a separation between electrodes of 0.2D.[17]

```
      $JOB
C     CALCULATIONS CORRESPONDING TO THE OPERATIONAL MODE A-A OF A
C     ------------------------------------------------------------
C     VARIABLE VOLTAGE RATIO ELECTROSTATIC LENS
C     ------------------------------------------------------------
C     THE CARDINAL POINTS CORRESPONDING TO TWO EQUIDIAMETER CYLINDERS
C     SEPARATED BY A SPACING OF 0.20 ARE STORED IN ARRAY (XI) WHERE
C     I=1...98.  EACH ELEMENT OF THE ARRAY (XI) CONTAIN THE CARDINAL
C     POINTS CORRESPONDING TO A VOLTAGE RATIO AND THE VOLTAGE RATIO
C     ITSELF.
      DIMENSION FM1(98),F1(98),FM2(98),F2(98),V(98)
      DO 1 I=1,98
      READ(5,10) DATA1,DATA2,DATA3,DATA4,DATA5
      FM1(I)=-DATA1
      F1(I)=-DATA2
      FM2(I)=DATA3
      F2(I)=DATA4
      V(I)=DATA5
   10 FORMAT(F6.2,2F9.2,F10.2,F9.2)
    1  CONTINUE
      WRITE(6,30)
   30 FORMAT(1X,'VF/V1' ,3X,'V2/VF',3X,'MAGN.',5X,'V2/V1')
C     THE LENTH L=C.
      C=4.
C     THE TRIAL AND ERROR METHOD IS ACCOMPLISHED USING TWO DO-LOOPS.
      DO 3 J=1,98
      DENO=2.*C-F2(J)
C     THE FACTOR 2 MULTIPLYING THE LENGTH  C IS DUE TO DATA NORMA-
C     LIZATION (GIVEN IN TERMS OF THE RADIUS OF THE CYLINDERS).
      IF(DENO) 8,8,8
    8 CONTINUE
C     THE MAGNIFICATION OF THE FIRST STAGE HAS BEEN CALLED AUA AND
C     THE MAGNIFICATION OF THE SECOND STAGE HAS BEEN CALLED AUA
      AUA=FM2(J)/DENO
      PA=C
C     THE OBJECT AND IMAGE DISTANCES OF THE FIRST STAGE HAVE BEEN CALLED
C     PA AND QA. AND THE OBJECT AND IMAGE OF THE SECOND STAGE HAVE BEEN
C     CALLED PD AND QD. THIS NOMENCLATURE HAS BEEN USED FOR THE
C     THREE OPERATIONAL MODES.  BUT IN EACH CASE THEIR EXPRESSIONS ARE
C     DIFFERENTS.
      QA=.5*(F1(J)+FM1(J)*AUA)
      DO 5 L=1,98
      QD=C
      AUD=(2.*C-F2(L))/FM2(L)
      IF(AUD)4,4,12
   12 CONTINUE
      PD=.5*(F1(L)+FM1(L)/AUD)
      S=ABS(PD)+ABS(QA)
      AUT=AUD*AUA
      VT=V(J)*V(L)
C     THE VALUE OF S IS COMPARED WITH THE VALUE GIVEN TO  L2
      IF(ABS(S-3.) .LE. .01) GO TO 6
      GO TO 4
    6 WRITE(6,20) V(J),V(L),AUT,VT
   20 FORMAT(1X,3(F5.2,3X),3X,F7.3)
    4 CONTINUE
    5 CONTINUE
    2 CONTINUE
    3 CONTINUE
    7 CONTINUE
      STOP
      END
```

```
      $JOB
      C     CALCULATIONS CORRESPONDING TO THE OPERATIONAL MODE A-D OF A
      C     ------------------------------------------------------------
      C     VARIABLE VOLTAGE RATIO ELECTROSTATIC LENS
      C     ------------------------------------------------------------
      C     THE CARDINAL POINTS CORRESPONDING TO TWO EQUICIAMETER CYLINDERS
      C     SEPARATED BY A SPACING OF 0.2D ARE STORED IN ARRAY (XI) WHERE
      C     I=1...99.  EACH ELEMENT OF THE ARRAY (XI) CONTAIN THE CARDINAL
      C     POINTS CORRESPONDING TO A VOLTAGE RATIO AND THE VOLTAGE RATIO
      C     ITSELF.
 1          DIMENSION FM1(98),F1(98),FM2(98),F2(98),V(99)
 2          DO 1 I=1,98
 3          READ(5,10) DATA1,DATA2,DATA3,DATA4,DATA5
 4          FM1(I)=-DATA1
 5          F1(I)=-DATA2
 6          FM2(I)=DATA3
 7          F2(I)=DATA4
 8          V(I)=DATA5
 9     10   FORMAT(F5.2,2F9.2,F10.2,F9.2)
10     1    CONTINUE
11          WRITE(6,30)
12     30   FORMAT(1X,'VF/V1' ,3X,'V2/VF',3X,'MAGN.',5X,'V2/V1')
      C     THE LENTH L=C.
13          C=4.
      C     THE TRIAL AND ERROR METHOD IS ACCOMPLISHED USING TWO DO-LOOPS.
14          DO 3 J=1,98
15          DENO=2.*C-F1(J)
      C     THE FACTOR 2 MULTIPLYING THE LENGTH  C IS DUE TO DATA NORMA-
      C     LIZATION (GIVEN IN TERMS OF THE RADIUS OF THE CYLINDERS).
16          IF(DENO) 2,2,8
17     8    CONTINUE
      C     THE MAGNIFICATION OF THE FIRST STAGE HAS BEEN CALLED AUA AND
      C     THE MAGNIFICATION OF THE SECOND STAGE HAS BEEN CALLED AUA
18          AUA=FM1(J)/DENO
19          PA=C
      C     THE OBJECT AND IMAGE DISTANCES OF THE FIRST STAGE HAVE BEEN CALLED
      C     PA AND QA. AND THE OBJECT AND IMAGE OF THE SECOND STAGE HAVE BEEN
      C     CALLED PD AND QD. THIS NOMENCLATURE HAS BEEN USED FOR THE
      C     THREE OPERATIONAL MODES.  BUT IN EACH CASE THEIR EXPRESSIONS ARE
      C     DIFFERENTS.
20          QA=.5*(F2(J)+FM2(J)*AUA)
21          DO 5 L=1,98
22          QD=C
23          AUD=(2.*C-F1(L))/FM1(L)
24          IF(AUD)4,4,12
25     12   CONTINUE
26          PD=.5*(F2(L)+FM2(L)/AUD)
27          S=PD+QA
28          AUT=AUD*AUA
29          VT=V(J)/V(L)
      C     THE VALUE OF S IS COMPARED WITH THE VALUE GIVEN TO  L2
30          IF(ABS(S-3.) .LE. .01) GO TO 6
31          GO TO 4
32     6    WRITE(6,20) V(J),V(L),AUT,VT
33     20   FORMAT(1X,3(F5.2,3X),3X,F7.3)
34     4    CONTINUE
35     5    CONTINUE
36     2    CONTINUE
37     3    CONTINUE
38     7    CONTINUE
39          STOP
40          END
```

```
      $JOB
C     CALCULATIONS CORRESPONDING TO THE OPERATIONAL MODE D-D OF A
C     ------------------------------------------------------------
C     VARIABLE VOLTAGE RATIO ELECTROSTATIC LENS
C     ------------------------------------------------------------
C     THE CARDINAL POINTS CORRESPONDING TO TWO EQUIDIAMETER CYLINDERS
C     SEPARATED BY A SPACING OF 0.2D ARE STORED IN ARRAY (XI) WHERE
C     I=1,..,98.  EACH ELEMENT OF THE ARRAY (XI) CONTAIN THE CARDINAL
C     POINTS CORRESPONDING TO A VOLTAGE RATIO AND THE VOLTAGE RATIO
C     ITSELF.
      1     DIMENSION FM1(98),F1(98),FM2(98),F2(98),V(98)
      2     DO 1 I=1,98
      3     READ(5,10) DATA1,DATA2,DATA3,DATA4,DATA5
      4     FM1(I)=-DATA1
      5     F1(I)=-DATA2
      6     FM2(I)=DATA3
      7     F2(I)=DATA4
      8     V(I)=DATA5
      9  10 FORMAT(F6.2,4F9.2,F10.4,F9.2)
     10   1  CONTINUE
     11     WRITE(6,30)
     12  30 FORMAT(1X,'VF/V1',3X,'V2/VF',3X,'MAGN.',5X,'V2/V1')
C          THE LENGTH L=C.
     13     C=4.
C          THE TRIAL AND ERROR METHOD IS ACCOMPLISHED USING TWO DO-LOOPS.
     14     DO 3 J=1,98
     15     DENO=2.0C-F2(J)
C          THE FACTOR 2 MULTIPLYING THE LENGTH  C IS DUE TO DATA NORMA-
C          LIZATION (GIVEN IN TERMS OF THE RADIUS OF THE CYLINDERS).
     16     IF(DENO)12,2,6
     17   6 CONTINUE
C          THE MAGNIFICATION OF THE FIRST STAGE HAS BEEN CALLED AUA AND
C          THE MAGNIFICATION OF THE SECOND STAGE HAS BEEN CALLED AUA
     18     AUA=FM2(J)/DENO
     19     PA=C
C          THE OBJECT AND IMAGE DISTANCES OF THE FIRST STAGE HAVE BEEN CALLED
C          PA AND QA, AND THE OBJECT AND IMAGE OF THE SECOND STAGE HAVE BEEN
C          CALLED PD AND QD. THIS NOMENCLATURE HAS BEEN USED FOR THE
C          THREE OPERATIONAL MODES.  BUT IN EACH CASE THEIR EXPRESSIONS ARE
C          DIFFERENTS.
     20     QA=.5*(F1(J)+FM1(J)*AUA)
     21     DO 5 L=1,98
     22     QD=C
     23     AUD=(2.0C-F1(L))/FM1(L)
     24     IF(AUD)4,4,12
     25  12 CONTINUE
     26     PD=.5*(F2(L)+FM2(L)/AUD)
     27     S=PD+QA
     28     AUT=AUD*AUA
     29     VA=1./V(J)
     30     VD=1./V(L)
     31     VT=VA*VD
C          THE VALUE OF S IS COMPARED WITH THE VALUE GIVEN TO  L2
     32     IF(ABS(S-3.) .LE. .01) GO TO 6
     33     GO TO 4
     34   6 WRITE(6,20) VA,VD,AUT,VT
     35  20 FORMAT(1X,3(F5.2,3X),3X,F7.3)
     36   4 CONTINUE
     37   5 CONTINUE
     38   2 CONTINUE
     39   3 CONTINUE
     40   7 CONTINUE
     41     STOP
     42     END
```

Table 2. Cardinal Points Corresponding to Two Equidiameter Cylinders. The separation between the electrodes is 0.2D.

f/R	F/R	f'/R	F'/R	V'/V
68.25	75.61	83.59	75.45	1.50
21.98	26.27	31.08	26.00	2.00
12.05	15.32	19.05	14.97	2.50
8.11	10.88	14.04	10.45	3.00
6.08	8.55	11.38	8.06	3.50
4.84	7.13	9.73	6.59	4.00
4.06	6.19	8.81	5.60	4.50
3.49	5.52	7.81	4.89	5.00
3.08	5.01	7.21	4.35n	5.50
2.75	4.63	6.74	3.93	6.00
2.50	4.32	6.37	3.60	6.50
2.12	3.87	5.81	3.08	7.00
2.02	3.82	5.68	2.98	7.50
1.98	3.69	5.59	2.89	8.00
1.86	3.54	5.41	2.71	8.50
1.75	3.42	5.25	2.56	9.00
1.66	3.30	5.11	2.43	9.50
1.58	3.21	4.99	2.32	10.00
1.44	3.04	4.79	2.11	10.50
1.39	2.98	4.70	2.03	11.00
1.34	2.91	4.63	1.98	11.50
1.29	2.85	4.56	1.87	12.00
1.25	2.80	4.46	1.81	12.50
1.21	2.75	4.43	1.74	13.00
1.20	2.73	4.41	1.73	13.50
1.17	2.71	4.38	1.69	14.00
1.14	2.67	4.33	1.63	14.50
1.11	2.63	4.29	1.51	15.00
1.08	2.60	4.25	1.57	15.50
1.05	2.57	4.21	1.49	16.00
1.06	2.54	4.17	1.45	16.50
0.98	2.48	4.14	1.41	17.00
0.97	2.47	4.11	1.37	17.50
0.96	2.46	4.08	1.34	18.00
0.94	2.44	4.06	1.31	18.50
0.92	2.41	4.03	1.27	19.00
0.91	2.39	4.01	1.24	19.50
0.89	2.37	3.99	1.21	20.00

Table 2.-continuation

0.88	2.36	3.97	1.19	20.50
0.86	2.34	3.95	1.16	21.00
0.85	2.32	3.97	1.11	21.50
0.83	2.31	3.91	1.11	22.00
0.82	2.29	3.90	1.09	22.50
0.81	2.28	3.88	1.06	23.00
0.80	2.26	3.87	1.04	23.50
0.79	2.25	3.86	1.02	24.00
0.78	2.24	3.84	1.00	24.50
0.77	2.23	3.83	0.89	25.00

LIST OF REFERENCES

1. G. D. Yarnold and H.C. Bolton, J. Sci. Instr. 40 (1949) 38.
2. G. A. Harrower, Rev. Sci. Instr. 26 (1955) 850.
3. J.D.H. Eland and C.J. Danby, J. Phys. E. (J. Sci. Instr.) 1 (1968) 406.
4. A.L. Hughes and J.H. McMillen, Phys. Rev. 35 (1929) 291.
5. P. Marmet and L. Kerwin, Can. J. Phys. 38 (1960) 787.
6. M.E. Rudd, Ph.D. thesis, University of Nebraska, 1962.
7. C.E. Kuyatt and M.E. Rudd, Bull. Amer. Phys. Soc. 8, No. 4 (1963) 336.
8. E.M. Purcell, Phys. Rev. 54 (1938) 818.
9. F.W. Aston, Phil. Mag. 38 (1919) 710.
10. H. Hafner, J. Arol Simpson, and C.E. Kuyatt, Rev. Sci. Instr. 39 (1968) 33.
11. F.R. Paolimi and G.L. Theodoridis, Rev. Sci. Instr. 38 (1967) 579.
12. H. Wollnik, Focusing of Charged Particles. Vol. II, Edited by A. Septier, (Academic Press, New York, 1967).
13. C.E. Kuyatt and J.A. Simpson, Rev. Sci. Instr. 38 (1967) 103.
14. R.F. Herzog, Phys. Z. 41 (1940) 18.
15. H. Wollnik and H. Ewald, Nucl. Instr. Methods 36 (1965) 93.
16. K.R. Spangenberg, Vacuum Tubes, (McGraw-Hill, New York, 1948).
17. A.B. El-Kareh, Electron Beams, Lenses and Optics. Vol. I (Academic Press, New York, 1970).
18. T.L. Bailey, Lectures on Ion Optics, given Jun-August 1976. University of Florida. (unpublished)

BIOGRAPHICAL SKETCH

Jose Manuel Perez was born in LA HABANA, Cuba, on August 18, 1948. He received a B.S. degree in physics from the University of Madrid (Spain) in 1974.